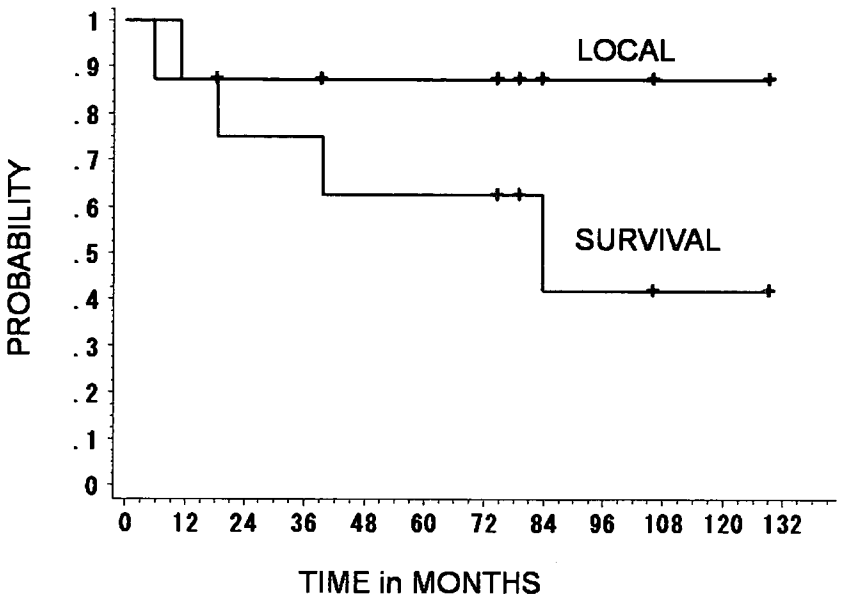

Fig. 2: Local control and survival curves of 8 patients in pilot study.

The 5 years and 10 years local control rate was 87.5% (S.E.: 11.7%) and 87.5% (S.E.: 11.7%)(Fig. 2). One meningioma patient died of local relapse at 11.1 month, one chordoma patient died of multiple lung metastases at 18.6 month, one metastatic adenocarcinoma patient died of multiple lung metastases at 39.5 month and one chordoma patient died of skip lesion of cervical bone at 83.9 months. The 5 year and 10 year survival rate was 62.5% (S.E.: 17.1%) and 41.7% (S.E.: 20.5%)(Fig. 2).

Result of Phase I/II Dose Escalation Study

The phase I/II dose escalation study for skull base tumor was started on April 1997. Till the August of 2003, a total of 29 patients were entered into the study. They were consisted of 16 cases with chordoma, 6 cases of meningioma, 5 cases of chondrosarcoma, one case of olfactory neuroblastoma and one case of giant cell carcinoma. Their age ranged from 21 to 68 years with median of 47 years. There were 11 male and 18 female patients. All patients were treated by 16 fractions for 4 weeks and total dose was 48.8 GyE for 4 patients, 52.8 GyE for 6 patients, 57.6 GyE for 10 patients and 60.8 GyE for 9 patients. Used number of ports was 2 ports for 11 patients, 3 ports for 16 patients and 4 ports for 2 patients (Table 1).

In acute skin reaction, one patient, who had 492.6 cm3 CTV and was treated by 48.0 GyE, showed grade 3

Phase I/II Study (Skull Base)

		Number of Port			
Dose	total	1	2	3	4
48.0 GyE	4	0	1	3	
52.8	6	0	2	4	
57.6	10	0	6	4	
60.8	9	0	2	5	2
TOTAL	29	0	11	16	2

Table 1: The number of ports in carbon ion radiotherapy for skull base tumor (phase I/II study).

reaction (Fig. 3). There was no other grade 3 or higher acute skin reaction (Table 2). In acute mucosal reaction, one patient, who had 345.6 cm3 CTV and was treated by 57.6 GyE, showed grade 3 reaction. There was no other grade 3 or higher acute mucosal reaction (Table 3). There was no observation of acute brain and spinal cord. In late reactions, observed maximum reactions were 1) grade 1 skin reaction in 4 patients, 2) grade 1 mucosal reaction in 2 patients, 3) grade 2 brain reaction in 2 patients, and 4) no reaction in the spinal cord.

Five year local control showed 79% in 16 chordoma patients, 80% in 6 meningioma patients and 100% in 5 chondrosarcoma patients (Fig.4). Five year over all survival showed 87% in chordoma, 83% in meningioma and 60% in chondrosarcoma (Fig. 5).

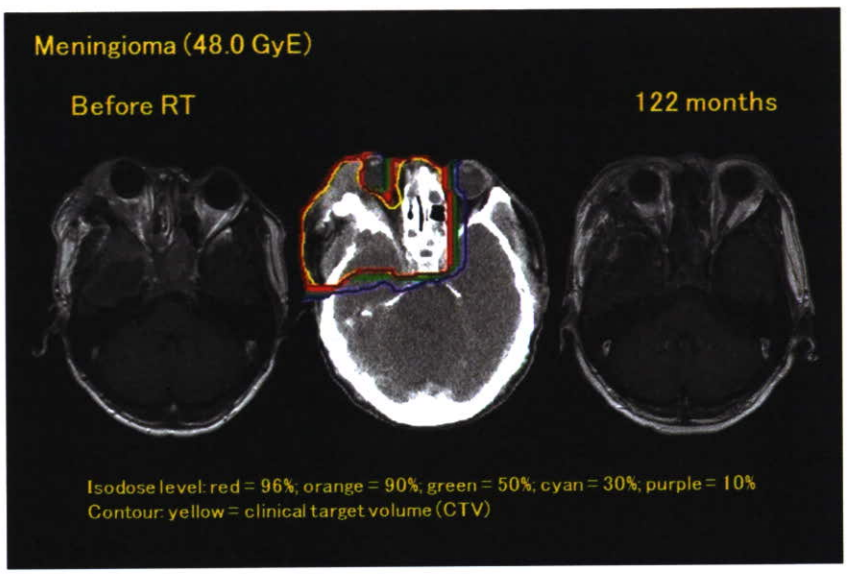

Fig. 3: Meningioma patient treated by 48 GyE/16fractions/4 weeks. The patient had 492.6 cm3 CTV and showed grade 3 skin reaction.

Phase I/II Study (Skull Base)

Acute Reaction (Skin)

		Grade				
Dose	total	0	1	2	3	4
48.0 GyE	4	1	2	0	1	
52.8	6	2	2	2		
57.6	10	4	6			
60.8	9	1	7	1		
TOTAL	29	8	17	3	1	0

Table 2: Acute skin reaction in phase I/II study for skull base tumor.

Phase I/II Study (Skull Base)

Acute Reaction (Mucosa)

		Grade				
Dose	total	0	1	2	3	4
48.0 GyE	4	4	0	0		
52.8	6	4	0	2		
57.6	10	4	5	0	1	
60.8	9	4	5			
TOTAL	29	16	10	2	1	0

Table 3: Acute mucosal reaction in phase I/II study for skull base tumor.

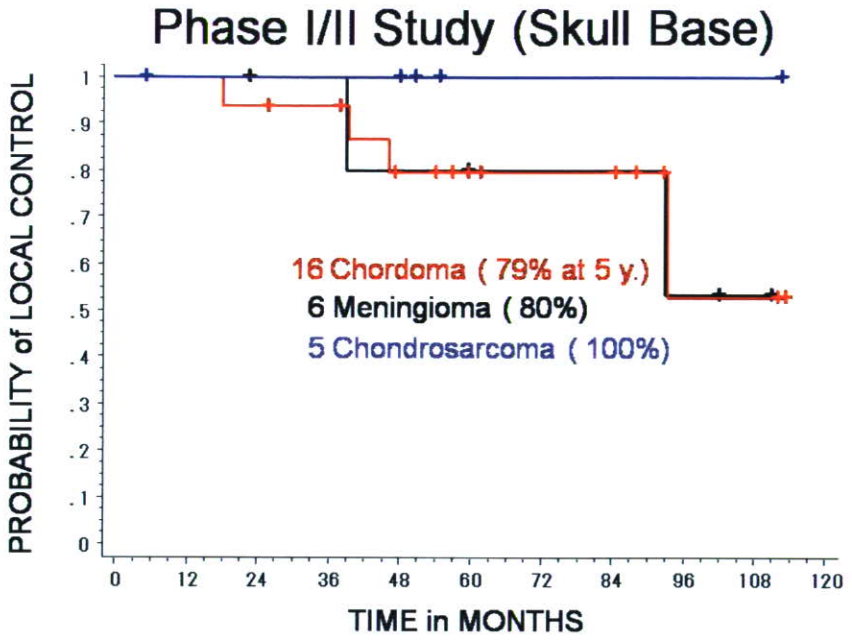

Fig. 4: Local control curves of 16 chordoma, 6 meningioma and 5 chondrosarcoma patients (Phase I/II study).

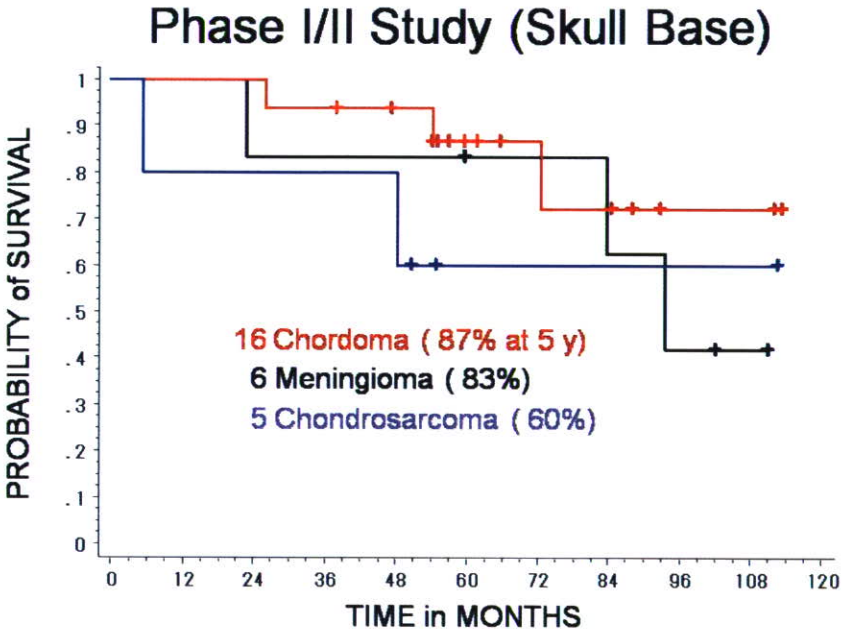

Fig. 5: Survival curves of 16 chordoma, 6 meningioma and 5 chondrosarcoma patients (Phase I/II study).

Preliminary Results of Phase II Study

From the April of 2004, a phase II study has been started for the skull base tumor. Till the July of 2007, a total of 18 patients were treated by a fractionation method of 60.8 GyE (3.8 GyE fraction dose) through 16 fractions for 4 weeks. Adding the patients who were treated by 60.8 GyE in the phase I/II study between the September of 2002 and the August of 2003, a total 27 patients were analyzed in this sesstion There were 19cases of chordoma, 5 cases of chondrosarcoma and 2 cases of olfactory neuroblastoma. Their age ranged from 16 to 78 years with median age of 52 years. There were 13 male and 14 female patients. Twenty out of 27 patients were treated by shrinkage field after 38 GyE through 10 fractions. CTV1 for initial 10 fractions ranged from 4 to 247 cm3 with median volume of 73 cm3 and CTV2 for followed 6 fractions ranged from 4 to 187 cm3 with

median volume of 53 cm3.

In the acute reactions, observed maximum reactions were one patient with grade 2 skin reaction and 3 patients with grade 2 mucosal reaction. There were no reactions of the brain and the spinal cord. In the late reaction, only one patient showed grade 1 brain reaction and there were no other grade 1 or higher normal tissue reactions.

Follow up periods of 27 patients ranged from 7 to 63 months with median of 38 months and there was no local relapse till the time of analysis (Fig. 6). One out of 19 chordoma patients died of liver dysfunction at 8.7 month. Three out of 5 chondrosarcoma patients died of 1) metastasis of the distant cervical vertebrae at 4.2 month, 2) bleeding from tumor bed at 5.4 month and 3) pneumonia at 48.4 month. All of these 4 patients were confirmed as having no local relapse at the expired time. Overall survival curves are shown in Figure 7.

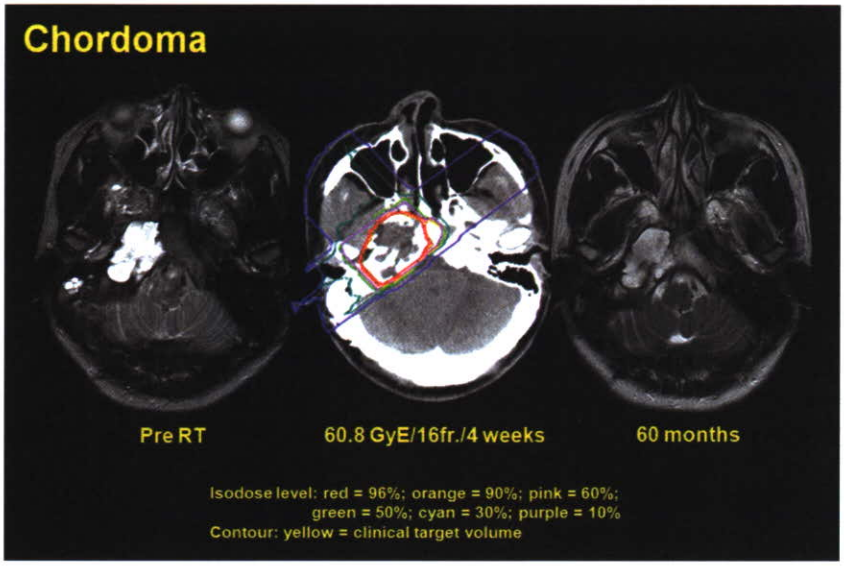

Fig. 6: Chordoma patient treated by 60.8 GyE/16 fractions/4 weeks. There is no re-growth of the tumor 60 months after therapy.

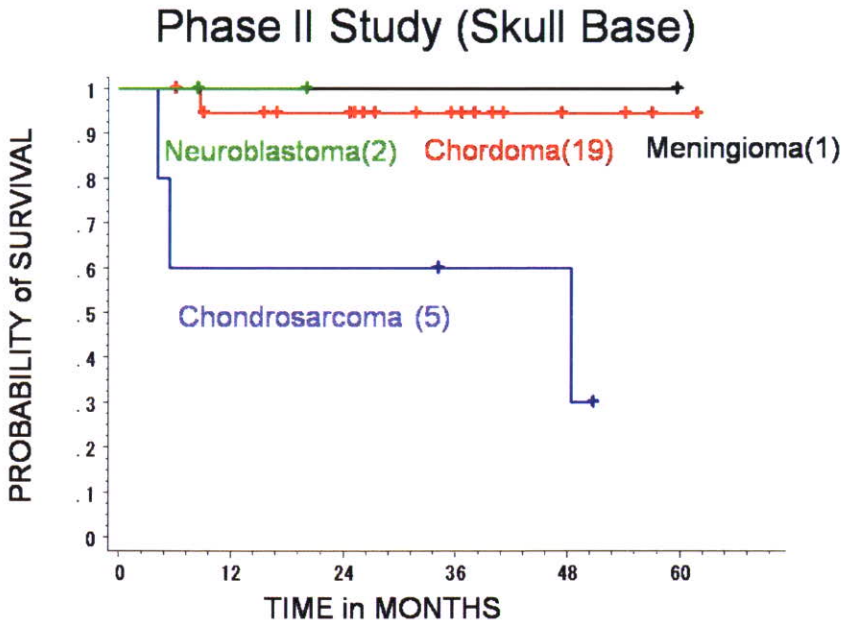

Fig. 7: Survival curves of 19 chordoma, 5 chondrosarcoma, 2 neuroblastoma and one meningioma patients (treated by 60.8 GyE in phase I/II + II study).

Discussion

Observed normal tissue reaction of phase II study is acceptable. Therefore, there will be some possibility of higher total dose than 60.8 GyE in NIRS study. Even if local control rate is 100% at present time and follow up periods is short, there will need careful and reliable follow up study of skull base patients for future total dose alternation.

Conclusion

Dose escalation study for skull base tumor concluded that 60.8 GyE/16 fractions/4 weeks is recommended dose for skull base tumor because of good local control rate.

With multi portal irradiation, normal tissues showed mild reaction and there is no severe morbidity of important organs.

References

1. Mendenhall WM, Mendenhall CM, Lewis SB, et al. Skull base chordoma. Head Neck. 2005; 27: 159-65.
2. Jereczek-Fossa BA, Krengli M, Orecchia R. Particle beam radiotherapy for head and neck tumors: radiobiological basis and clinical experience. Head Neck. 2006; 28:750-60.
3. Debus J, Hug EB, Liebsch NJ, et al. Brainstem tolerance to conformal radiotherapy of skull base tumors. Int J Radiat Oncol Biol Phys. 1997; 39:967-75.
4. Noel G, Feuvret L, Calugaru V, et al. Chordomas of the base of the skull and upper cervical spine. One hundred patients irradiated by a 3D conformal technique combining photon and proton beams. Acta Oncol. 2005;44:700-8.
5. Weber DC, Rutz HP, Pedroni ES, et al. Results of spot-scanning proton radiation therapy for chordoma and chondrosarcoma of the skull base: the Paul Scherrer Institut experience. Int J Radiat Oncol Biol Phys. 2005; 63: 401-9.
6. Schulz-Ertner D, Nikoghosyan A, Hof H, et al. Carbon ion radiotherapy of skull base chondrosarcomas. Int J Radiat Oncol Biol Phys. 2007; 67: 171-7.
7. Schulz-Ertner D, Karger CP, Feuerhake A, et al. Effectiveness of carbon ion radiotherapy in the treatment of skull-base chordomas. Int J Radiat Oncol Biol Phys. 2007; 68: 449-57.

Inter-comparison between GSI and NIRS for Biological Effectiveness of Carbon Ions

Akiko Uzawa [*1], Koichi Ando[*1#], Sachiko Koike [*1], Yoshiya Furusawa [*1], Yoshitaka Matsumoto [*1], Nobuhiko Takai [*1], Ryoichi Hirayama [*1], Masahiko Watanabe [*1], Michael Scholz [*2], Thilo Elsässer [*2] and Peter Peschke [*3]

[*1]: Research Center of Charged Particle Therapy, National Institute of Radiological Sciences, Chiba, Japan
[*2]: Biophysics, Gesellschaft für Schwerionenforschung, Darmstadt, Germany
[*3]: Radiation Oncology, Deutsches Krebsforschungszentrum, Heidelberg, Germany

[#] Corresponding author: ando@nirs.go.jp

INTRODUCTION

A phase I/II clinical study on carbon ion radiotherapy started at National Institute of Radiological Sciences (NIRS), Chiba, Japan in 1994. A total of nearly 3000 patients have been treated with HIMAC synchrotron by Year 2006, and are analyzed for toxicity and local tumor response (1). Clinical studies of carbon ion radiotherapy using SIS synchrotron also started at Gesellschaft für Schwerionenforschung (GSI), Darmstadt, Germany in 1997, and large effort has been paid to treat chordoma of the skull base (2). Clinical outcome of these two institutions has been well recognized and attract a lot of attention from worldwide. Therapeutic effectiveness of carbon ion beams depends on factors including physics and biology. Different from photon beams, carbon ion beams are biologically heterogeneous along with the beam path, due to change of linear energy transfer or LET. This heterogeneity is most prominent at Spread-Out Bragg peak or SOBP that targets deep-seated tumors in the patient body. As the SOBP of Chiba/HIMAC therapy is provided by use of a scatterer (3), projectile particles should be more fragmented within the SOBP than that of GSI/SIS which is made by changing beam energy and do not use any scatterer (4). It is therefore important to compare biological effectiveness of carbon ion beams between NIRS/HIMAC and GSI/SIS. We here have intercompared between the two beams using gut crypt survivals, and reported that the two beams are biologically identical to each other after single and daily-fractionated irradiation as well.

MATERIALS and METHODS

Animals:

C3H/He female mice 10 to 12 weeks old were used. Mice were produced in specific pathogen free facilities at NIRS, and moved 2-3 days before start of irradiation to conventional environment in either NIRS or GSI. Anesthesia with ketamine and xyladine was used during irradiation. Mice were kept in a Lucite jig especially designed for gut irradiation, and they received horizontal beams. For each dose, either 3 or 4 mice were used.

Irradiation:

Carbon ions were accelerated to 290 MeV/u by HIMAC and SIS synchrotrons, and spread out to 6-cm width. The SOBP profile for the SIS synchrotron used in the experiment was adjusted to be the same as the SOBP profile being used for therapy at Chiba (3), and was different from that being used for therapy at Darmstadt. Using different thickness of tissue-equivalent absorbers, mouse jejunum was placed at 3 different positions within the 6-CM SOBP, i.e., middle position, 2-cm upstream form the middle position and 2-cm downstream form the middle position. Dose rates for HIMAC and SIS beams depended on irradiation position, and were

approximately 3 Gy/min and 1 Gy/min, respectively. Mice received either single dose irradiation or 3 fractionated doses with a fixed interval of 24 hr for 3 days.

Endpoint:

Crypt survivals were histologically measured. Jejunum was removed and fixed in formalin 3.5 days after irradiation. Histology preparations were made, and H&E staining was used to count microscopically the number of crypts surviving and regenerating. For non-irradiated control, the number of crypts per circumference section was between 120 and 145. Experiments were repeated 2 or 3 times for each synchrotron facilities, and the data obtained from each were combined for use. Obtained on survival curves were two iso-effect doses of D30, and D10, the doses required to reduce survivals to 30 and 10 crypts, respectively. Isoeffect doses were used to compare biological effectiveness between the two facilities.

RESULTS

Figure 1 shows physical depth dose distribution of carbon ion beams used in the present study. Jejunum was irradiated at 3 positions indicated by arrows. Jejunum located 7 mm depth from abdominal skin surface, which was measured by a range absorber method. As shown in figure 2, mice were placed in a Lucite jig and received

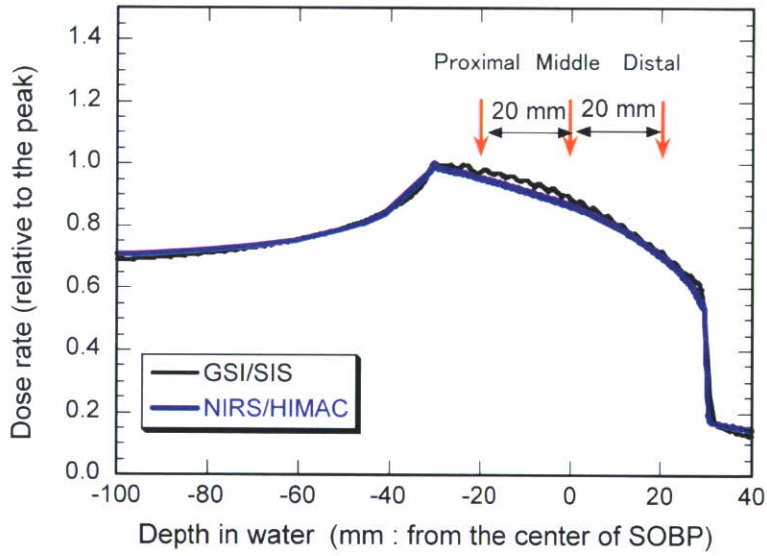

Figure 1 Depth dose distribution of Carbon-ion beams with a 6-cm SOBP
Arrows indicate three positions of gut irradiated with carbon ions.

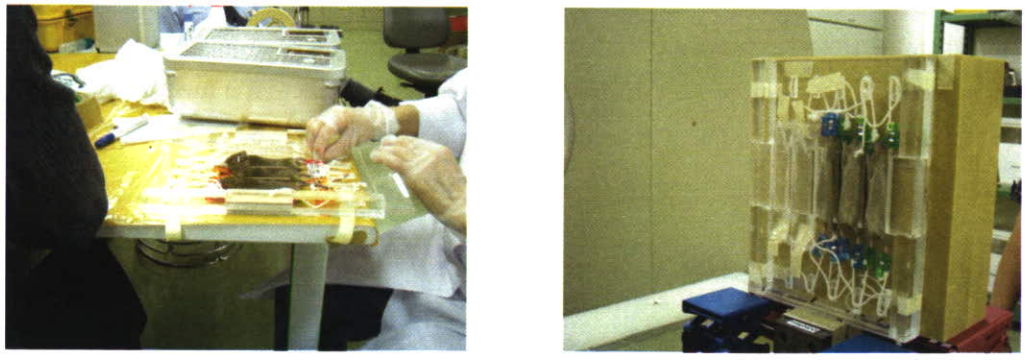

Figure 2 Mice immobilized in a jig.
Left panel: Receiving an IP injection of ketamine and xylazine, mice were placed in a Lucite jig. Hands and feet were picked by clothespins with strings. Right panel: Horizontal beams passed through a Lucite plate (4 mm thick) and abdominal wall before reaching to jejunum.

horizontal beams. Carbon ions pass through a 4-mm thick Lucite plate and abdominal wall before reaching to jejunum. First, physical doses of carbon 6-CM SOBP at various positions were measured (figure 3 A). Changing thickness of binary filters, doses sharply drop at the distal fall-of of the SOBP. Within 2 mm from the initial drop, doses decreased to nearly 1/10. The middle position of this drop was made by a use of 129 mm thick of binary filter. Second, jejunum crypt survivals were measured at various positions within the same 6-Cm SOBP. After a fixed dose of 10 Gy at a position made by 109 mm thick of binary filter, number of crypt survived this dose was 1.0 (figure 3B). Number of crypts gradually increased when thickness of binary filter increased from 114 mm, and reached to 130, almost an unirradiated level , at 123 mm thick. This increase is due to decrease of physical doses at the distal fall-off. What was different from physical fall-off was that the range of crypts increase was 9 mm and wider than the range of dose decrease. This indicates that jejunum was not flat to the horizontal beam, and partly bending back and forth in body. The middle position of the crypt drop was made by a use of 118 mm thick of binary filter. Subtracted 118 mm form 129, resulting 11 mm includes thickness of both the 4mm thick Lucite and abdominal wall, thickness of which could easily be calculated as 7 mm (the water equivalent thickness of 4 mm Lucite is 4.64 mm) .

Figure 4 shows crypt survivals after single and fractionated dose of carbon-ion irradiation. The left panel is for proximal positions at NIRS and GSI, and indicates very similar dose response relationship between the two facilities. This similarity is also observed fort the middle (middle panel) and the distal (right panel) positions.

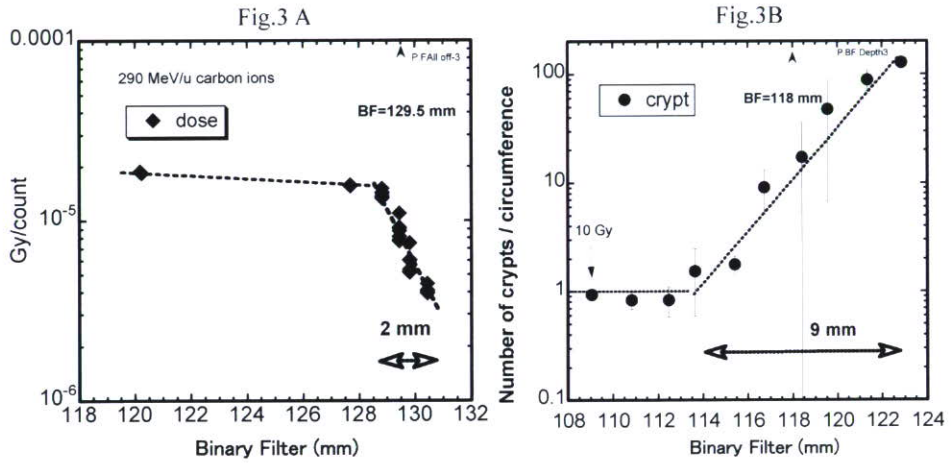

Figure 3 A method used to determine depth of jejunum in body.
290 MeV/u Carbon-ion beams with 6-cm SOBP were used. Left panel: Physical dose fall-off, right panel: Crypt survivals at the fall-of.

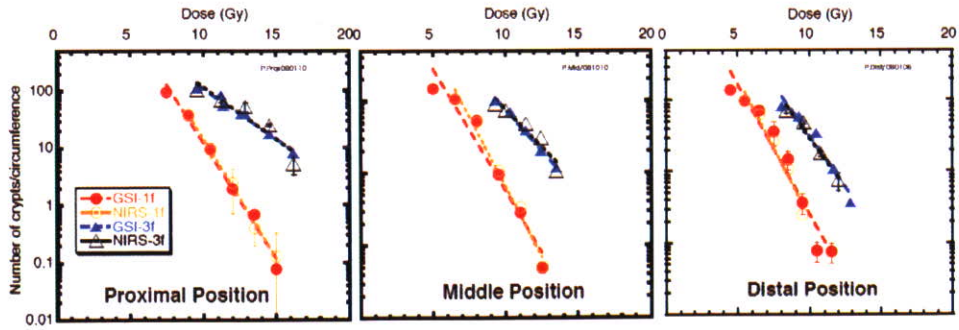

Figure 4 Crypt survivals after irradiation with carbon ions
Single doses for GSI were shown as red, closed circles, while single doses for NIRS as orange, open circles. For 3 fractions, GSI data were shown as blue, closed triangles, while NIRS data as open black triangles. Bar is standard deviation.

DISCUSSION and CONCLUSION

We here presented and compared between GSI and NIRS for gut crypt survivals after irradiation with 6-cm carbon-ion SOBP profiles. Comparing isoeffect doses for single irradiation, a ratio of GSI to NIRS (GSI/NIRS) of carbon ions at D_{30} were 1.02, 1.05 and 1.01 for proximal , middle and distal position, respectively. , while the ratio of GSI/NIRS at D_{10} were 1.02, 1.03 and 1.00 for proximal , middle and distal position, respectively. Comparing isoeffect doses for fractionated carbon ions, the ratio at D_{30} were 1.02, 1.00 and 0.99 for proximal , middle and distal position, respectively, while the ratio at D_{10} were 0.98, 0.98 and 0.99 for proximal , middle and distal position, respectively. When we averaged these values, difference between GSI and NIRS beams is 1 %. We conclude that no difference between the two synchrotron facilities of carbon-ion beams was detected by the gut crypt survivals method, an in vivo dosimetry.

ACKNOWLEDGEMENTS

We are grateful to Prof.Gerhard Kraft, Dr.Sylvia Ritter, Dr.Suo Sakata and Dr.Ryonfa Lee for their help to conduct experiments. The animals involved in these studies were procured, maintained and used in accordance with the Recommendations for Handling of Laboratory Animals for Biomedical Research, compiled by the Committee on the Safety and Handling Regulations for Laboratory Animal Experiments, NIRS. This report is partly supported by the Special Coordination Funds for Research Project with Heavy Ions at the National Institute of Radiological Sciences-Heavy-ion Medical Accelerator in Chiba (NIRS-HIMAC).

References

1. Hirohiko TSUJII, Junetsu MIZOE, Tadashi KAMADA et al. (2006) Clinical Results of Carbon Ion Radiotherapy at NIRS, J.Radiat, Res. 48: A1-A13.
2. Schulz-Ertner D, Karger CP, Feuerhake A, et al. (2007) Effectiveness of carbon ion radiotherapy in the treatment of skull-base chordomas, Int J Radiat Oncol Biol Phys. ;68(2): 449-57
3. Tatsuaki Kanai, Masahiro Endo, Shinichi Minohara, et al. (1999) Biophysical characteristics of HIMAC clinical irradiation system for heavy-ion radiation therapy, Int.J.Radiation Oncology.Biol.Phys. 44(1), 201-210,
4, Oliver JAKEL, Daniela SCHULZ-ERTNER and Jurgen DEBUS (2007) Specifying Carbon Ion Doses for Radiotherapy: The Heidelberg Approach , J.Radiat, Res. 48: A87-A95

Relative Biological Effectiveness (RBE) of Carbon Ions in the Normal Central Nervous System (CNS).

Peter Peschke[1], Christian P. Karger[2], Michael Scholz[3], Juergen Debus[4], Peter Huber[1,4]

[1] Clinical Cooperation Unit Radiation Oncology, DKFZ Heidelberg, Germany
[2] Dept. of Medical Physics in Radiation Oncology, DKFZ Heidelberg, Germany
[3] Dept. of Biophysics, GSI Darmstadt, Germany
[4] Dept. of Clinical Radiology, University of Heidelberg, Germany

Introduction

Higher precision and an improved biological effectiveness were the main driving forces in experimental radiotherapy for the past 100 years. Particle radiotherapy using protons and carbon ions closely meet these demands, because ion beams have millimeter precision and an inverse depth-dose profile with an increase of the dose with depth. In addition to these physical advantages, heavy charged particles such as carbon ions exhibit an increased relative biological effectiveness (RBE) in the Bragg peak relative to the plateau region. While several medical facilities exploit energetic protons to treat deep-seated tumors, the use of carbon ions is limited to two hospital based facilities in Japan and a pilot project in Germany at GSI. The first dedicated European clinical heavy-ion therapy (HIT) facility in Heidelberg (Germany) will soon be open for patient treatment. In Europe, an active beam scanning technique is used for dose delivery. Compared with passive beam delivery techniques favored in Japan, beam scanning allows for dose conformation not only at the distal but also at the proximal edge of the tumor for each field [1]. An important consequence of the beam scanning technique with heavy ions is the necessity to calculate tumor and normal tissue RBEs separately for each point within the complete treatment field. Yet, one has to keep in mind that although ion beams exhibit a previously unattained precision in dose delivery, there will always be small volumes of normal tissue in the high-dose volume. These might be normal tissue in the beam entrance channels, especially those close to the target volume, as well as normal tissue in the target volume itself which cannot be spared for various reasons.

The determination of biological effective doses is done by use of the local effect model (LEM). Such biophysical models are required, because the RBE of ion beams exhibits a complex dependence on many physical and biological parameters such as beam energy and LET, penetration depth, dose level and the repair capacity of the tissue as well as on the selected biologic endpoint [2]. The LEM is implemented in the treatment planning system and enables the assignment of "individual" RBEs to each of the millions of voxels in a patient CT [3]. Pilot studies at GSI focused on radioresistant skull-base tumors, locally advanced adenoid cystic carcinomas and paraspinal tumors, which are difficult to treat, because a sufficient high dose often cannot safely be delivered in general with conventional radiation, due to the tolerance doses of neighboring radiosensitive normal tissues. Unfortunately, in most cases the radiation tolerance of these critical normal structures are not known precisely, because of uncertainties in the RBE of the carbon ions (^{12}C). To exploit the role of carbon ions for late complications in the normal central nervous system (CNS), normal rat brain as well as the rat spinal cord was used as a late effect model to determine the radiotolerance of photon and carbon ion irradiations.

Response of the normal rat brain.

In 1997 we have started our investigations with a study applying single doses of carbon ions and photons to the right frontal lobe of the normal rat brain. Animals were irradiated stereotactically at the right frontal lobe using an extended Bragg-peak with maximum doses between 15.2 and 29.2 Gy. Late changes in the normal brain, detected by T1- and T2-weighted magnetic resonance imaging (MRT) were taken as basis to calculate dose-response curves. For follow up, two biological end points were selected at 12, 14, 16 and 20 months: (A) any contrast enhancement in the brain after injection Gd-DTPA in T1-weighted MRI, and (B) any hyperintense signal in the brain in T2-weighted MRI.

Radiation-induced tissue alterations of the normal rat brain monitored by MRI exhibited a time-dependent progression up to 17 month post irradiation and remained stationary after that time. At 20 months the tolerance doses at the 50% effect probability level were 20.3 ± 2.0 Gy and 22.6 ± 2.0 Gy for changes in T1- and T2-weighted MRI, respectively [4]. The RBE, as calculated on the basis of a previous identical animal study with photons was 1.95 ± 0.2 and 1.88 ± 0.18 for T1- and T2-weighted MRI [5].

This study represented the first published quantitative analysis of carbon ion-induced late effects in the normal brain. Remarkable was the differential behavior of the selected biological endpoint: Beyond 17 months the MRI changes remained in a progressive state for photons, whereas the tolerance dose for carbon ions was already stationary. This situation lead to decreasing tolerance doses for photons and hence to some extend time-dependent RBE-values. No significant difference in RBE was found for the two MRI end points. Although the tolerance doses for the two MRI techniques were quite different, the RBE-values are nearly the same. Moreover, the comparison of our results with a parallel performed single dose study on carbon ion-induced myelitis of the rat spinal cord yielded a rather good agreement with respect to RBE. This holds in spite of the different tissue architecture and the different biological endpoints. The labor intensive treatment procedures with individually positioned animals in a stereotactic frame, the elaborative follow-up by MRI and the suboptimal biological endpoint supported the decision that for systematic measurements of normal-CNS complications the spinal cord might represent the more suitable model.

Tolerance of the rat spinal cord.

The cranial part of the spinal cord of the rat was irradiated with 1, 2, 6 or 18 fractions of photons or ^{12}C-ions, respectively. Plateau irradiations were performed in the entrance region of a 270 MeV/u Bragg-peak, while for the peak irradiations a 10 mm spread-out-Bragg-Peak of 140 MeV/u. was used. Animals were followed up for 300 days after irradiation for the onset of paresis grade II. Dose response curves were calculated for each irradiation experiment and D_{50}-values (dose at 50% complication probability) were determined. Based on these D_{50}-

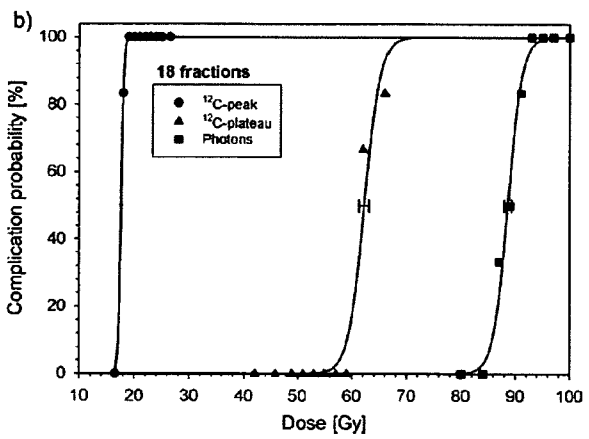

Fig. 1. Dose-response curves for late complications of the rat spinal cord after 18 consecutive fractions of carbon ions in a 10 mm spread-out Bragg peak (circles), in the entrance channel of 12C-ions (triangles) and photons (squares). (reprinted from [7] with permission from Elsevier)

values, the RBE and the related α/β-parameters were calculated. The measured RBE-values were compared with predictions of the local effect model (LEM).

The experimentally determined RBE-values for 1, 2, 6 and 18 fractions were 1.44±0.08, 1.37±0.05, 1.33±0.02 and 1.42±0.02 for the plateau- and 1.77±0.06, 2.17±0.06, 2.97±0.05, and 5.04±0.08 for the peak-irradiations. The respective predictions by the LEM were 1.14, 1.19, 1.37, and 1.72 for the plateau- and 1.28, 1.61, 2.35, and 3.80 for the peak irradiations. The α/s-values derived by logistic regression were 2.8±0.4 Gy for photons, 2.1±0.4 Gy for the plateau and 37.0±5.3 Gy for the peak-irradiations, respectively [6,7].

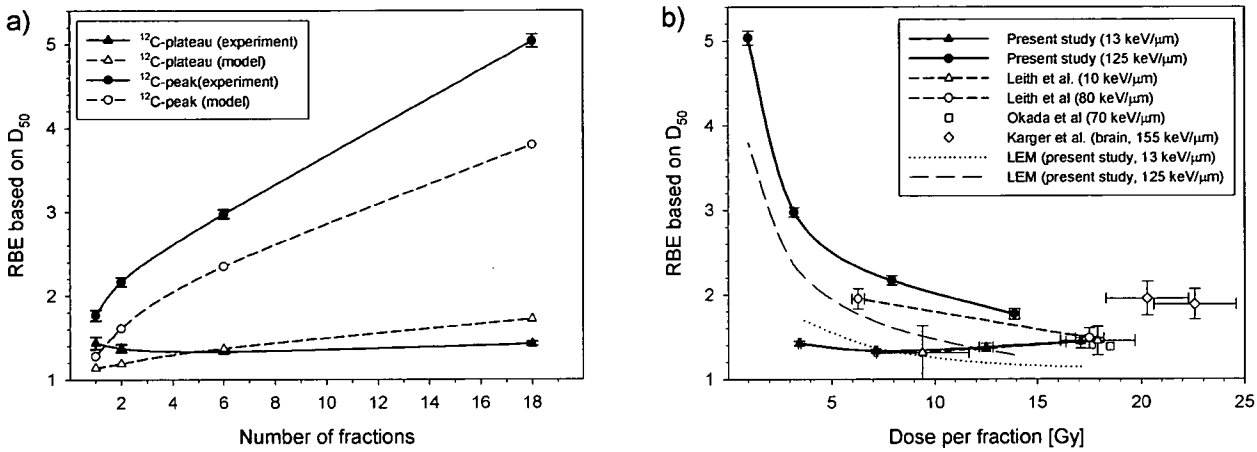

Fig. 2. Radiation-induced myelitis in the rat spinal cord: Dependence of the relative biological effectiveness (RBE) on fraction number (a) and dose (b). (reprinted from [7] with permission from Elsevier).

Carbon ion irradiations of the spinal cord are significantly more effective in the peak than in the plateau region. A significant fractionation effect was only found for the plateau-irradiations. For the peak irradiations, the LEM correctly describes the dose dependence of the RBE, although it generally underestimates the RBE by 25%. In the plateau region, overestimations of up to 20% were found for the clinically applied low doses per fraction. The experimental data contribute to the validation of the LEM and quantify the involved uncertainties

Discussion and Conclusion

As a complementation to experiments performed at NIRS focusing on early reacting normal tissues, we have directed our interest to late complications in the normal tissue of the CNS. In our hands, the spinal cord tissue model turned out to be a reliable system to exploit different radiation qualities, especially with respect to their role in late radiation effects. Up to now, only few experimental data on the RBE of carbon ions were available for the CNS. Morphological parameters were in the focus of normal brain studies. The effects of carbon-ion irradiation and X-irradiation on the development of rat brain were compared on the histological level showing that the effects of both carbon-ion irradiation and X-irradiation on the development of rat brain are similar in character. The effect of 1.5 Gy carbon-ion irradiation compares to that of 2.0 or 2.5 Gy X-irradiation [8]. Impact of heavy ions on postnatal mouse cerebella development have been described [9] showing in vivo evidence of more pronounced apoptotic cell death after carbon ion treatment. The pathogenesis of delayed encephalopathy in cats induced by carbon ions was characterized by a long-standing edema of the white matter due to vascular hyperpermeability, and the vascular dilatation seemed to be caused by a reduction in the vascular bed and/or hemoconcentration due to hyperpermeability [10].

The latency interval for the development of limb paralysis after the irradiation of the rat spinal cord with fractionated doses of charged particles in the plateau and Bragg-peak regions was first examined by Leith et al. and

Rodriguez et al. [11-13]. Their results showed a distinct decreased tissue tolerance in the high-LET Bragg-peak region. The RBE of high-LET beams of charged particles, for spinal cord injury, is known to be in the range of 1.2 to 3.0 [14,15] with the RBE being lower for single compared to fractionated doses [12]. This database is significantly extended by the present study, especially in the clinically relevant region of low doses per fraction. Moreover, the results clearly demonstrate that in vivo studies with well characterized biological endpoints are helpful contributions to better define the tolerance doses needed for normal tissues. The experimental data contributed to the validation of the LEM and helped to quantify the involved uncertainties.

In the course of the clinical pilot studies at GSI only a few tumor types have been treated, mostly brain, head-and-neck, and spinal cord cancers. One of the challenges for the upcoming new medical facilities, will be to verify if the rasterscan-based treatment can be successfully extended to a number of other tumor sites. As normal-tissue tolerance remains the limiting factor for a general extension to new tumor sites, it is for these sites that more information on normal-tissue response is urgently needed to minimize the risk associated with the treatment. Likewise, as a consequence of the physical and biological enhanced effectiveness, hypofractionation (large fraction sizes) is taken in consideration and in a number of cases patients have been treated with better tumor control than conventional therapy [16]. Systematic in vivo measurement combined with an radiobiology modeling of fractionation effects should help to answer the question to what extent a fractionation scheme remains its advantage in reducing the risk to normal tissue. Last but not least, studying the molecular mechanisms underlying carbon ion irradiation on normal tissues effects might not only help to understand clinical response but also might open new avenues for the development of interventional strategies for patients undergoing carbon ion therapy.

Acknowledgements:

We thank Alexandra Tietz, Uschi Schierbaum, Karin Leotta and Rainer Kuhnlein (DKFZ) for their excellent technical support. We also thank Dr. Rita Sanchez-Brandelik, University of Freiburg, Germany, Prof. Albert van der Kogel, Univ. Nijmegen, NL and Prof. Eric W. Hahn, U.T. Southwestern Medical School at Dallas, TX, USA for their help with the experimental set up and design of the study.

References

1. Kraft G. (2000) Tumor therapy with heavy charged particles. Prog. Part. Nucl. Phys. 45: S473.S544.
2. Scholz M., Kellerer A.M., Kraft-Weyrather W., Kraft G. (1997) Computation of cell survival in heavy ion beams for therapy. The model and its approximation. Radiat. Environ. Biophys. 36: 59-66, 1997.
3. Kramer M, Weyrather WK, Scholz M. (2003) The increased biological effectiveness of heavy charged particles: from radiobiology to treatment planning. Technol Cancer Res. Treat. 2: 427-436.
4. Karger CP, Munter MW, Heiland S, Peschke P, Debus J, Hartmann GH. (2002) Dose-response curves and tolerance doses for late functional changes in the normal rat brain after stereotactic radiosurgery evaluated by magnetic resonance imaging: influence of end points and follow-up time. Radiat. Res. 157: 617-625.
5. Karger CP, Debus J, Peschke P, Munter MW, Heiland S, Hartmann GH. (2002) Dose-response curves for late functional changes in the normal rat brain after single carbon-on doses evaluated by magnetic resonance imaging: influence of follow-up time and calculation of relative biological effectiveness. Radiat. Res. 158: 545-555.
6. Debus J., Scholz M., Haberer T., Peschke P., Jakel O., Karger C.P., Wannenmacher M. (2003) Radiation

tolerance of the rat spinal cord after single and split doses of photons and carbon ions. Radiat. Res. 160: 536-542.

7. Karger C.P., Peschke P., Sanchez-Brandelik R., Scholz M., Debus J. (2006) Radiation tolerance of the rat spinal cord after 6 and 18 fractions of photons and carbon ions: experimental results and clinical implications. Int. J.Radiat. Oncol. Biol. Phys. 66: 1488-1497.
8. Inouye M, Takahashi S, Kubota Y, Hayasaka S, Murata Y. (2000) Similarity between the effects of carbon-ion irradiation and X-irradiation on the development of rat brain. J Radiat Res (Tokyo).41: 303-311.
9. Kinoshita C., Yaoi T., Nojima K., Fushiki S. (2003) The effects of heavy ion particles on the developing mirine cerebellum, with special reference to cell death. Acta Histochem Cytochem. 36: 145-151.
10. Okeda R, Okada S, Kawano A, Matsushita S, Kuroiwa T. (2003) Neuropathology of delayed encephalopathy in cats induced by heavy-ion irradiation. J Radiat Res (Tokyo). 44: 345-352.
11. Leith,T., Woodruff K.H., Howard J., Lyman T., Smith P., Lewinsky B.S. (1977) Early and late effets of accelerated charged particles on normal tissue. Int. J. Radiat. Oncol. Biol. Phys. 3: 103-108.
12. Leith J.T., McDonald M., Powers-Risius P., Bliven S.F., Howard J. (1982) Response of rat spinal cord to single and fractionated doses of accelerated heavy ions. Radiat. Res. 89: 176-193.
13. Rodriguez A., Alpen E.L., DeGuzman R.J. Irradiation of rat thoraco-lumbar spinal cord with fractionated doses of helium and neon ions. In Proceedings of the 8th International Congress of Radiation Research, Vol. 1, pp. 249.
14. Geraci J.P. and Mariano M.S. (1994) Relationship between dose and the latent period for radiation myelopathy in rats. Radiat. Res. 140: 340-346.
15. Okada S., Okeda R., Matsushita S. Kawano A. (1998) Histopathological and morphometric study of the late effects of heavy-ion irradiation on the spinal cord of the rat. Radiat. Res. 150: 304-315.
16. Tsujii H, Mizoe J, Kamada T, et al. (2007) Clinical Results of Carbon Ion Radiotherapy at NIRS. J Radiat Res (Tokyo). 48 Suppl A: A1-A13.

Corresponding Author:
Peter Peschke, Ph.D.
Department of Radiation Oncology German Cancer Research Center Im Neuenheimer Feld 280
69120 Heidelberg, Germany
Email: P.Peschke@dkfz.de

産総研における線量標準の現状と今後

独）産業技術総合研究所計測標準研究部門量子放射科
放射線標準研究室　黒澤　忠弘

Corresponding: tadahiro-kurosawa@aist.go.jp

1．はじめに

当所では、X線・γ線の線量標準として、空気カーマ・照射線量を供給している。線量の強度としては、環境・防護・診断・治療領域をカバーしている。また放射線防護のために、β線による組織吸収線量標準も設定を行い、2006年度から校正を開始した。本報告では、これらX線・γ線・β線の線量標準に関して概説し、最後に今後の計画について簡単に紹介する。

2．X線標準

産総研ではX線照射施設として、管電圧10kV～50kVの軟X線照射室、管電圧40kV～300kVの中硬X線照射室の二つを有している。X線の線質を表す指標として次式に示すQI値（Quality Index）を用いている。

$$QI = \frac{E_{eff}}{E_{tube}} \qquad (1)$$

ここで、Etubeは管電圧（kV）、Eeffは実効エネルギー（keV）で、実効エネルギーは基準電離箱による電流測定によって得られた半価層から求めている。中硬X線では、管電圧が40, 50, 60, 75, 100, 125, 150, 175, 200, 225, 250kV、QI値は0.4, 0.5, 0.6, 0.7, 0.8, 0.9が、また軟X線では管電圧10, 15, 20, 30, 40, 50kV、QI値が0.4, 0.5, 0.6, 0.7, 0.8の条件で照射場を設定している。

照射線量の絶対測定を行うために、軟、中硬X線とも自由空気電離箱を用いている。自由空気電離箱の概略図を図1に示す。軟X線では空気による減衰の影響が大きいことから、小型の自由空気電離箱を用いている。自由空気電離箱で照射線量を測定する場合に基準となる位置は規程面と呼ばれ、電離箱のX線入射口の絞りの内側に設定されている。規程面の面積と集電極のビーム軸方向の長さとの積を空気体積といい、この容積が感度に比例する。

測定した電流に対して以下に上げる様々な補正等を行い、照射線量を求めている。[1]

1）空気質量の算出：測定時における気温、気圧による空気密度の補正
2）湿度補正：空気中の湿度による電離量の補正
3）再結合補正：イオン再結合により飽和電流が得られないための補正
4）空気減衰補正：規程面と電流を測定している集電極中心との間の空気層によるX線の減衰を補正
5）電子損失補正（Kel）：電離箱内で生じた高速電子が電極等にエネルギー付与した分の補正
6）散乱線補正（Ksc）：電離箱内で生成された二次光子による電離量の補正
7）入射口散乱･透過補正:入射口側面によって生成された散乱線による電離量の補正、またエッジ部分を透過した光子による電離量の補正

上記の5)、6)、7）に対する補正係数は測定から求めることは非常に困難であることから、シミュレーションによる計算によって補正係数を評価している。図2にEGSコード［2］によって求められた補正係数の例を示す。[3]

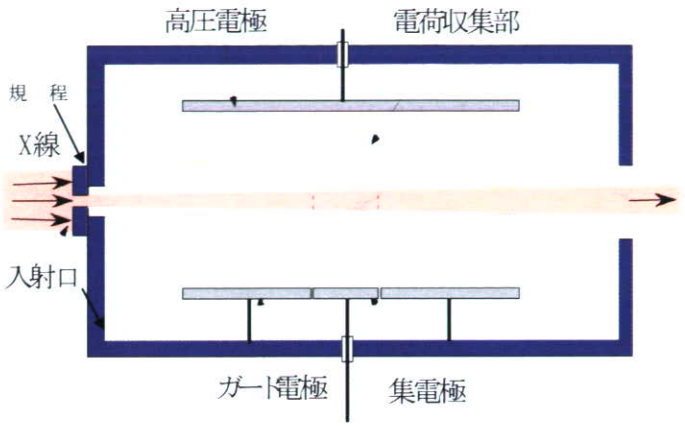

図１　自由空気電離箱の構造

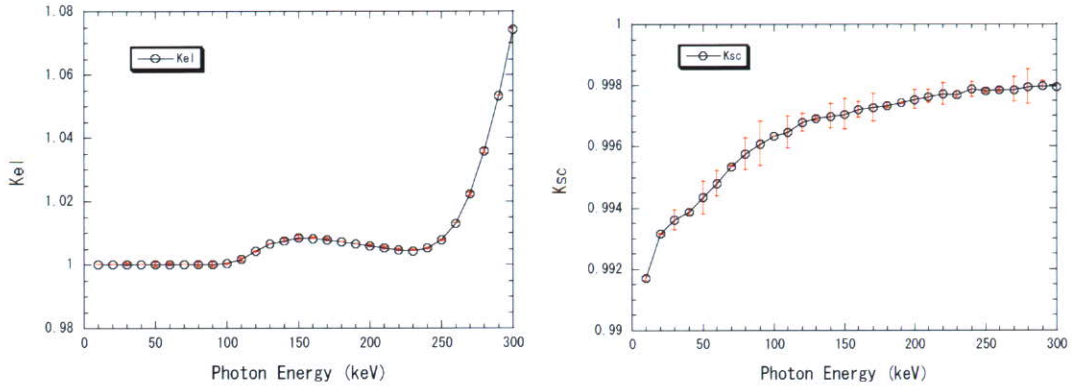

図２　中硬Ｘ線用自由空気電離箱の電子損失、散乱線補正係数。単色エネルギー光子に対する結果である。

３．　γ線標準

γ線照射施設として、小γ線源照射室及び大γ線源照射室の二つがある。照射に使用している線源は以下のものである。

小γ線源照射室：Cs-137---　222GBq,　18.5GBq,　1.85GBq

Co-60----　185GBq,　18.5GBq,　3.7GBq

大γ線源照射室：Cs-137---　34TBq

Co-60----　134TBq

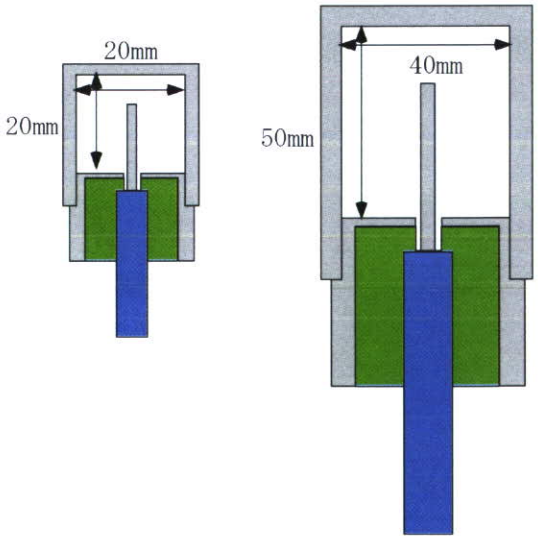

図３　グラファイト壁空洞電離箱の概略図。右側の空洞容量は約60ml，左側は約6ml。

γ線照射線量の測定には、グラファイト壁空洞電離箱を用いている。これはBragg-Grayの空洞理論を基にしている。線量率の違いにより、図３に示すような空洞容積の異なる２種類の円筒型空洞電離箱を用いて絶対測定を行っている。[4, 5]

空洞電離箱の場合も、測定された電離電流に様々な補正、換算を行って照射線量を求めている。

１）空気質量の算出:測定時における気温、気圧による空気密度の補正

２）湿度補正：空気中の湿度による電離量の補正

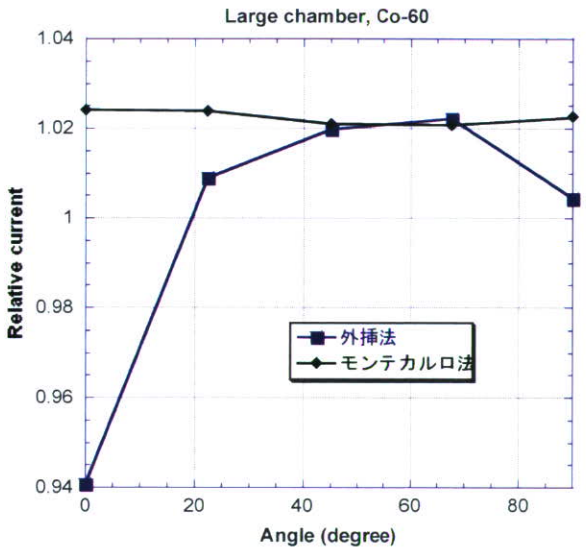

図４　電離箱の電離電流に対する外挿法とEGSコードによる壁補正後の照射角度依存

3）再結合補正：イオン再結合により飽和電流が得られないための補正
4）質量エネルギー吸収係数比：壁材のグラファイトから空気への換算
5）質量阻止能比：空洞内物質の空気からグラファイトへの電子阻止能の換算
6）ステム散乱補正：電離箱を支えているステムからの散乱線の寄与を補正
7）壁補正:電離箱壁によるγ線の減衰、また壁内で生成された散乱線を補正

1）～6）は、測定または評価されている物理定数から求めているが、7）に関しては、従来の測定法に問題があることが分かり、現在はシミュレーションによる計算によって評価している。その計算例として図４を示す。これは電離箱の設定角度を０度から90度まで変化させた場合の、従来の壁補正手法であった外挿法とシミュレーションによる壁補正を行った後の比較である。図からも明らかなように、電離箱の照射角度を変えると外挿法では補正が十分ではなく補正後の値が一定ではない。これは壁による減衰が角度によって異なるためで、シミュレーションによる補正を行うことによって値が一定となることが分かった。[6]

４．β線標準

β線組織吸収線量標準は旧電総研時に一度設定されたが［7］、照射装置、測定器とも老朽化し、近年では使用されていなかった。そこで、β線標準に関するISO規格［8］に準拠した照射装置、また絶対測定を行うための外挿電離箱を製作し、再設定を行った。

β線源としてはPm-147，Kr-85，Sr-90/Y-90の三種類で、照射場を均一にするために線源と基準位置の間にフラッタリングフィルターを設置している。図５に照射装置及び外挿電離箱の概略図を示

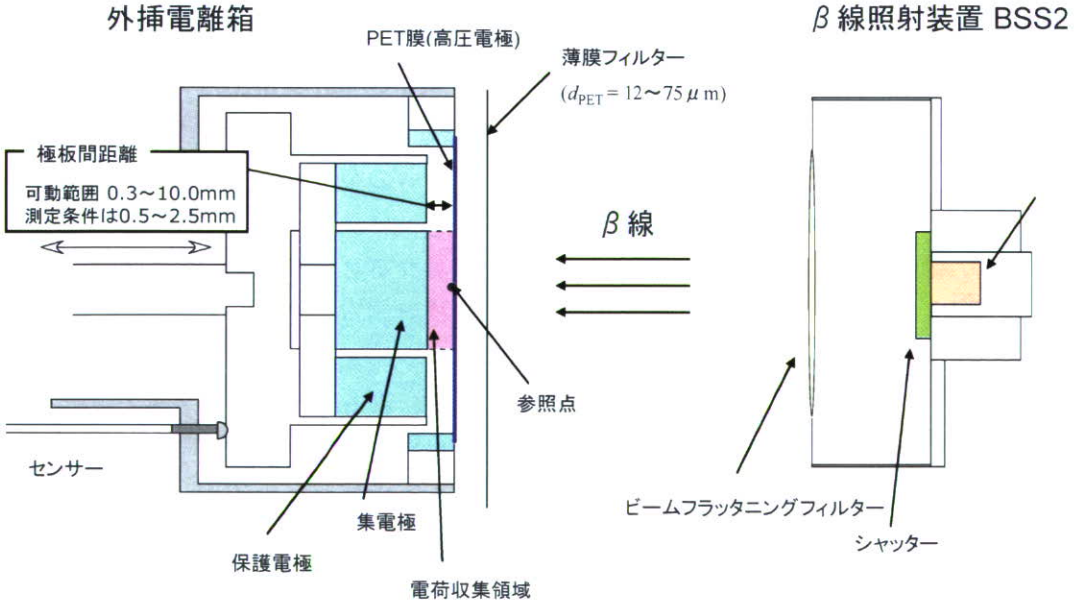

図５　外挿電離箱及び照射装置概略図

す。検出器前面はアルミコーティングされたPET膜で、電離箱の高電圧極となっている。集電極及び保護電極は可動式となっており、電極間隔を0.3mm～10mmまで変化させながら電離電流値を測定することが可能である。

外挿電離箱による7mg/cm^{2}深部の組織吸収線量率$\dot{D}$（0.07）は、電極間隔 l の関数としての電離電流値 $I(l)$ を用いて、次式により求める。

$$\dot{D}(0.07) = s_{t,a}\frac{\overline{W_0}}{e}\frac{1}{\rho_{a0}a}\left[\frac{\mathrm{d}}{\mathrm{d}l}KI(l)\right]_{l=0} \qquad (2)$$

ここで$_{st,a}$は、β線に対する組織と空気の平均質量阻止能比で、外挿電離箱で計測される電離箱内の空気吸収線量を、組織吸収線量に換算するための係数である。$(\overline{W_0}/e)$は、参照条件（気温20℃、大気圧1013hPa、相対湿度65％）における空気の平均のW値と素電荷の比で、電離箱で計測される電離電荷量を吸収エネルギーに変換するための係数である。aは集電極の実効的な面積で、ρ_{a0}は標準状態の空気の密度である。

$\left[\frac{\mathrm{d}}{\mathrm{d}l}KI(l)\right]_{l=0}$ は電流値増加量を極板間隔増加量で割った商の極板間隔0における極限であり、Kは各種の補正係数の積を表している。補正された電流値$KI(l)$は電極間隔 l に対して大まかには比例関係を示す。測定により得た$KI(l)$に対して二次式でフィッティングを行い、得られた二次式に基づいて $\left[\frac{\mathrm{d}}{\mathrm{d}l}KI(l)\right]_{l=0}$ を求める。

5．放射線標準の今後の計画について

5．1　水吸収線量標準の開発

医療、特に放射線治療分野の基準となっているCo-60に対する水吸収線量標準の開発を進めている。水吸収線量の定義としては、単位質量あたりの水に吸収されるエネルギーであり、J/kg (=Gy)である。本研究では、吸収されるエネルギーを測定するためにグラファイトカロリーメータ［9］を用いている。図6にその概略図を示す。熱量測定部となるコアと、その周りを覆うジャケット、シールドからなる。コア、ジャケット、シールドとも温度測定用サーミスター、温度調整用ヒーターが内臓されている。外部からの熱雑音を小さくするために、各領域の間には真空層を設けている。Co-60 γ線による温度上昇率は、一分の照射で約1m℃と非常に小さいため、サーミスターの微小な抵抗の変化を測定する必要がある。本システムでは、交流ブリッジ回路による変化量の測定を行っている。

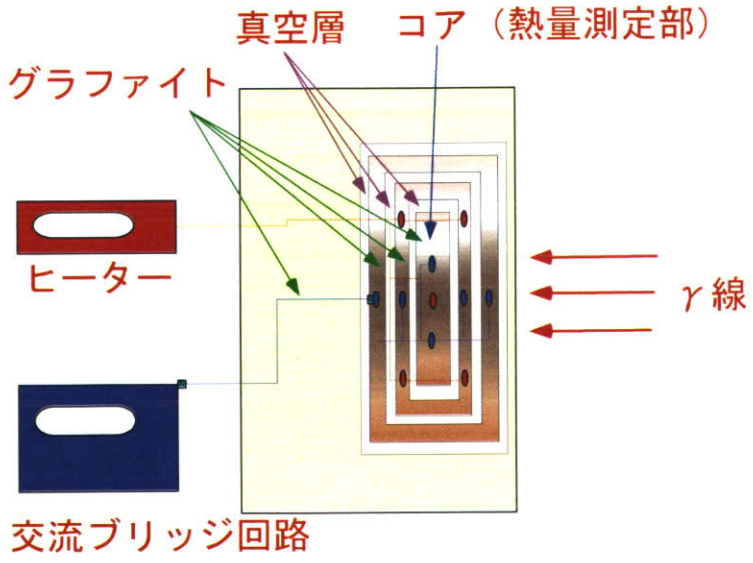

図6　グラファイトカロリーメータ概略図

カロリーメータによって測定される量はグラファイト吸収線量であり、水吸収線量への変換が必要となる。図７に変換のための概念図を示す。グラファイトカロリーメータで評価したグラファイト吸収線量を、一度仲介器である空洞電離箱に同一のファントム中で値付けする。これを水中のファントムに移し、水中でのグラファイト吸収線量を評価する。グラファイトから水吸収線量へは、質量エネルギー吸収係数によって換算を行い、最終的に水中のある深さにおける水吸収線量を評価することができる。校正を行う際には、水ファントム中に被校正機器を設置し測定を行うことになる。

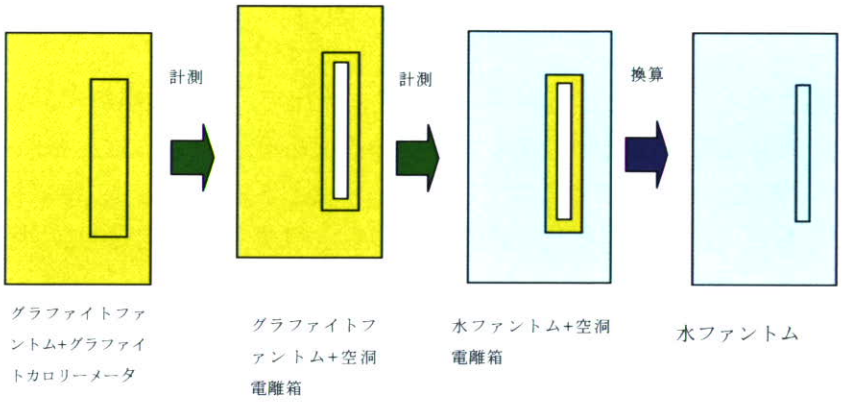

図７　グラファイトカロリーメータから水吸収線量評価のためのステップ概念図

５．２　マンモグラフィ線質の開発

マンモグラフィを用いた乳癌検診が急速に普及しており、その品質管理のためにその線質に対応した標準の供給が重要となっている。産総研では低エネルギーのＸ線発生装置としてはタングステンターゲットの管球を所有しているのみであったが、社会のニーズに合わせるため、新たにモリブデンターゲットのＸ線管球を導入した。現在は照射装置の特性評価を行っており、2008年度中にはIEC61267に示されている線質を開発し供給を開始したいと考えている。

５．３　I-125小線源空気カーマ

小線源治療に用いられているI-125の基準線量は、線源から1m離れた位置での空気カーマ率となっている。線源はおよそ15MBqであることから、微小電流を測定する困難さがある。将来的には外挿型の自由空気電離箱による絶対測定を予定しているが、この治療の急速な普及により迅速な標準供給のニーズが高まっている。そこで日本アイソトープ協会と協力し、産総研の軟Ｘ線場において校正された大型の空洞電離箱を用いて校正する手法を開発している。

参考文献

[1] 松本健、直井次郎、電総研彙報, 47, 28(1983)
[2] H. Hirayama et.al., SLAC-R-730(2005)
[3] T.Kurosawa, N.Takata, Y.Koyama, J. Nucl., Sci. Technol., 42, 1077(2005)
[4] 高田信久、黒澤忠弘、小山保二、医用標準線量、7, 11(2002)
[5] Kurosawa T., Koyama Y., Takata N., 医用標準線量、6-2, 1 (2001)
[6] T.Kurosawa, N.Takata, Y.Koyama, Appl., Rad., Isot., 62, 805(2005)
[7] 松本健、崎原克彦、小山保二、電総研彙報、11, 73(1992)
[8] ISO 6980-2 (2004)
[9] Domen S.R., Lamperti J.P., A Heat-loss Compensated Calorimeter: Theory Design and Performance, J. Res. Nat. Bur. Stand. 78A, 1974

水吸収線量の標準線量計測

Dosimetry standards of absorbed dose to water

首都大学東京大学院　齋藤秀敏

Corresponding: saitoh@hs.tmu.ac.jp

1．はじめに

投与線量の変化に対して、腫瘍の局所制御率および正常組織の障害発生率は急峻に変化する。したがって、放射線治療において吸収線量は重要な管理項目の一つであり、５％[1] あるいは3.5%[2] の合成標準不確かさが目標値とされている。このことから、AAPM Report 13では５％の合成標準不確かさの要素として、ファントムを使用した吸収線量計測において2.5%、体内吸収線量計算において4.3%の標準不確かさを与えている[3]。

すべての放射線治療施設において正確な吸収線量評価を実施し、その線量評価が正しいことを保証するためには、

a）吸収線量の国家標準が確立していること。

b）国家標準にトレーサブルな線量校正サービスが提供されていること。

c）吸収線量計測のための標準プロトコルが提供されていること。

d）第三者による線量評価体制が整備されていること。

が、必須となる。

本項では、日本の放射線治療施設の現状を紹介し、線量校正および標準プロトコルの現状と今後などについて述べる。

（第三者評価については、峯村氏のページを参照いただきたい。）

2．日本の放射線治療の現状

日本における放射線治療の現状は、日本放射線腫瘍学会（JASTRO）データベース委員会放射線治療施設構造調査が２年に一度行うアンケート調査によって明らかにされている[4]。

図１は、1990年からの放射線治療を施行された全新患数および１治療施設あたりの新患数の平均値の年次変化を示している。1995年の調査では約73,000であった全新患数が、2005年の調査では約

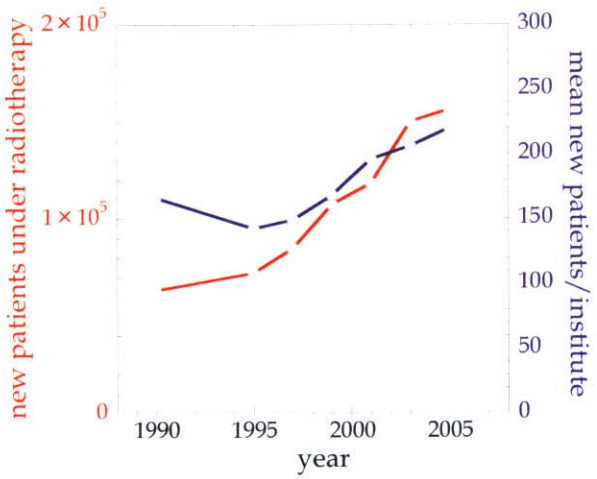

図１　放射線治療を受けた全新患数および一治療施設あたりの新患数の平均値の年次変化

Fig. 1 Change of new patients under radiotherapy